

SUPPLEMENTARY INFORMATION

Conformational Dynamics and Mechanical Properties of Biomimetic RNA, DNA, and RNA-DNA Hybrid Nanotubes: An Atomistic Molecular Dynamics Study

Ehsan Torkan¹, Mehdi Salmani-Tehrani^{1*}

¹ Department of Mechanical Engineering, Isfahan University of Technology, Isfahan, 84156-83111, Iran.

*Corresponding author. Email: Tehrani@iut.ac.ir.

Table S1 Genome sequences of RNA oligos of nanotubes. The genome sequences of DNA oligos are similar to those of RNA oligos, with the exception of the substitution of uracil (U) with thymine (T).

Strand number	Strand type	Genome sequence
1	Scaffold	5'-AUCCUGGUCGAGCUGGACGGCGACGUAAACGGCCACAAGU UCAGCGUGUCCGGCGA-3'
2	Scaffold	5'-CAUCUGCACCACCGGCAAGCUGCCCGUGCCCUGGCCACC CUCGUGACCACCCUGA-3'
3	Scaffold	5'-UCCAGGAGCGCACCAUCUUCUUAAGGACGACGGCAACU ACAAGACCCGCGCCGAG-3'
4	Scaffold	5'-AAGGGCAUCGACUUAAGGAGGACGGCAACAUCUGGG GCACAAGCUGGAGUACAA-3'
5	Scaffold	5'-GGACGGCAGCGUGCAGCUCGCCGACCACUACCAGCAGA ACACCCCAUCGGCGACG-3'
6	Scaffold	5'-CCGCCCUGAGCAAAGACCCCAACGAGAAGCGCGAUCAC AUGGUCCUGCUGGAGUUC-3'
7	Staple	5'-GCCGUCGUGCCGUCGUGGUAGUGGUCGAUCGCGCUU ACGUC-3'
8	Staple	5'-GCCGUCCGAACUCCCCAGGAU-3'
9	Staple	5'-UGGGGUCGUGUUCUCUCCUUGAAGUCGACGGGUCUCG GUGGU-3'
10	Staple	5'-UUGUACUUCCUGGAUCAGGGU-3'
11	Staple	5'-GAUGGGGUUUGCUCACACGCUGAACUUGAGCUUGCU GUAGUU-3'
12	Staple	5'-GGUCACGAGCUCGAAGCAGGACCAUGUGGCGAGCUGU GCCCC-3'
13	Staple	5'-CUCGGCGUGCCCUUCGUCGCC-3'
14	Staple	5'-GCCGUCCAGGGUGGAGAAGAUGGUGCGCCAGCUUG CACGCU-3'
15	Staple	5'-AGGAUGUCCUUGAGCCAGGGCACGGGUCGGCCGUUU CUCGU-3'
16	Staple	5'-GCAGAUGUCGCCGGAGGGCGG-3'

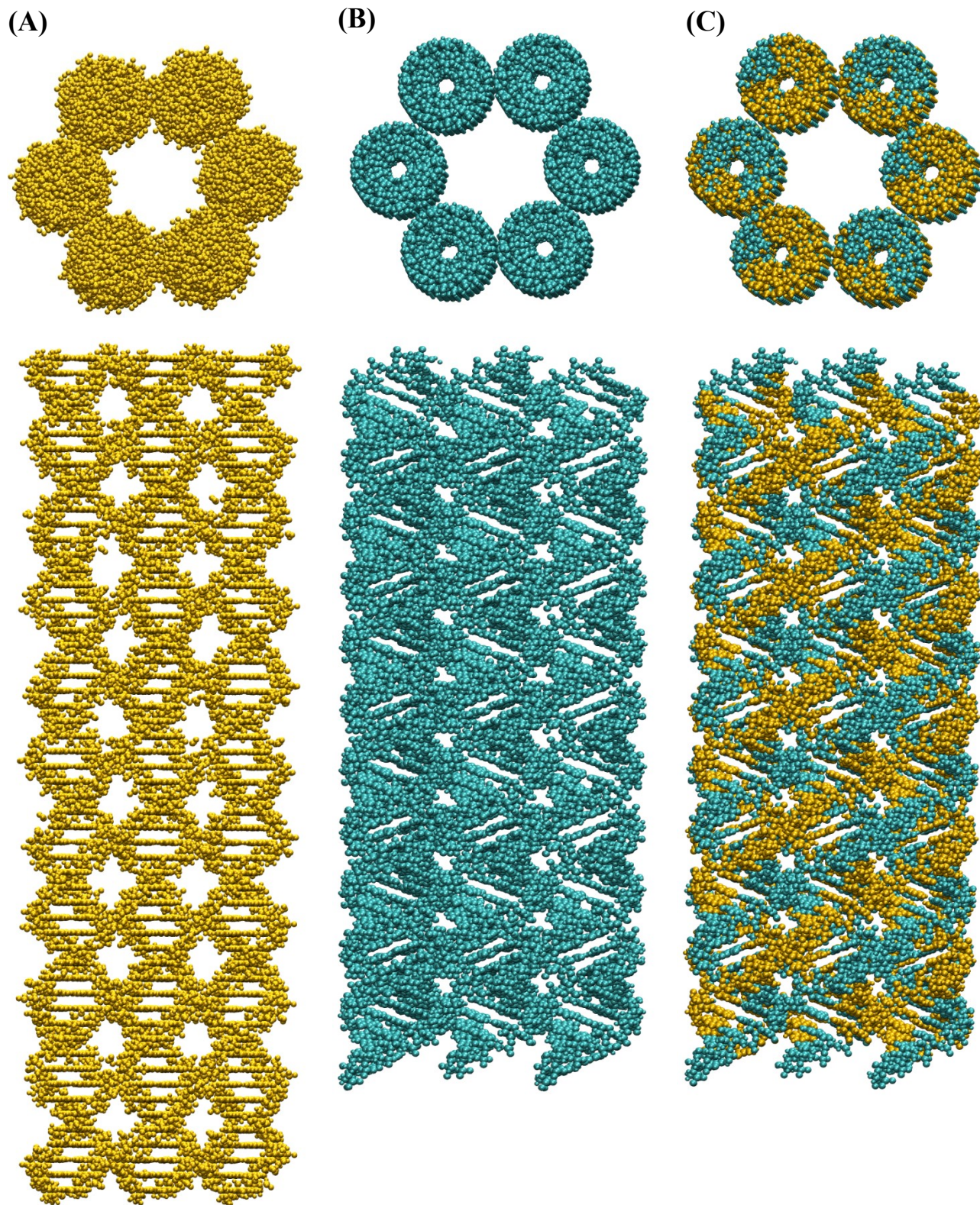


Figure S1 Top and side views of the initially built models of (A) DNT, (B) RNT, and (C) RDHNT.

Table S2 Details of the simulated systems in equilibrium MD simulations.

Structure	Box size (nm ³)	No. of base pairs	No. of water molecules	No. of Na ⁺ molecules	No. of atoms total (nanotube)
DNT	10×10×22	336	64311	656	214865(21276)
RNT	10.5×10.5×19	336	61084	656	205484(21576)
RDHNT	10.5×10.5×19	336	61196	656	205721 (21477)

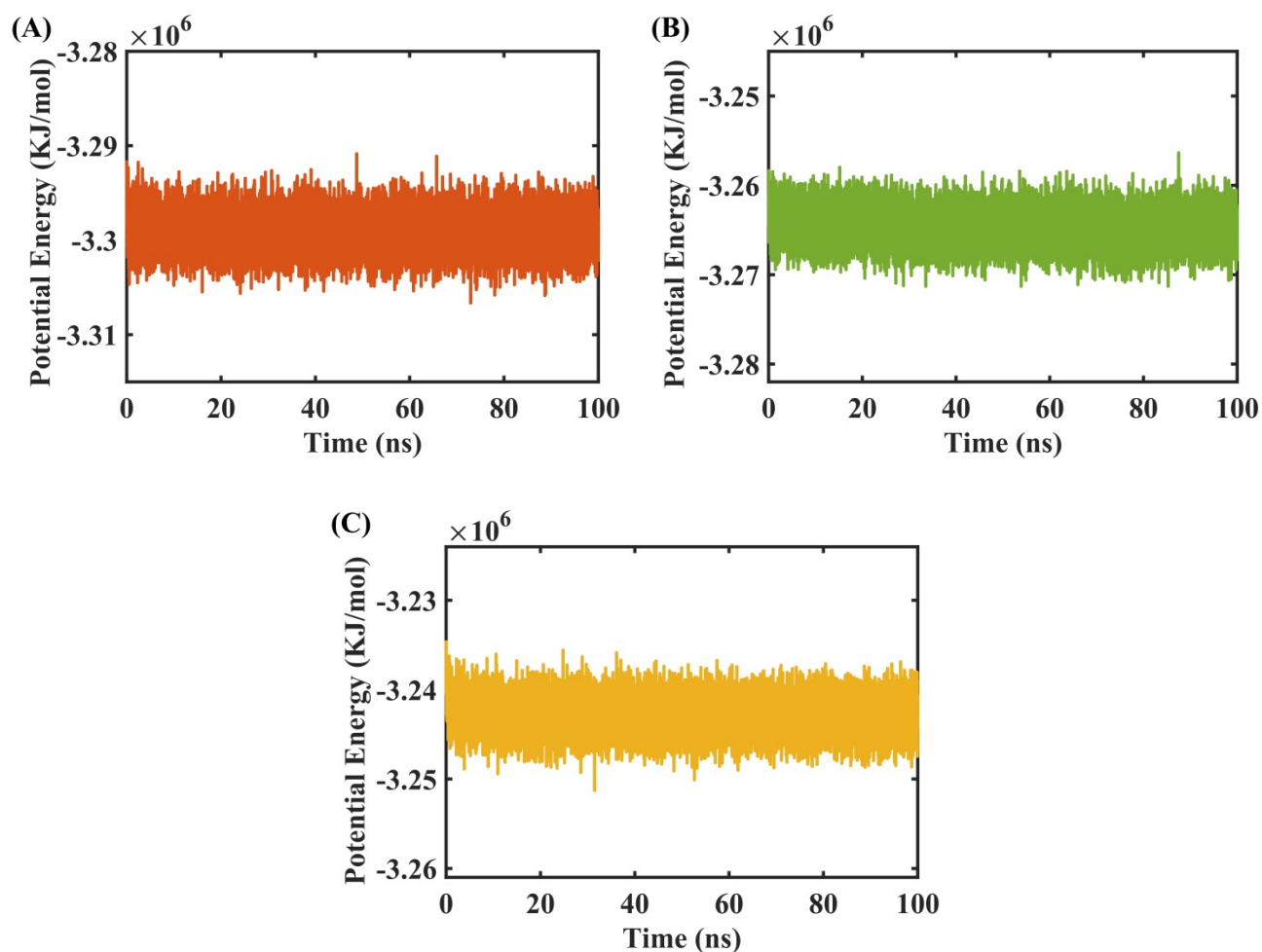


Figure S2 Potential energy of systems containing (A) DNT, (B) RNT, and (C) RDHNT.

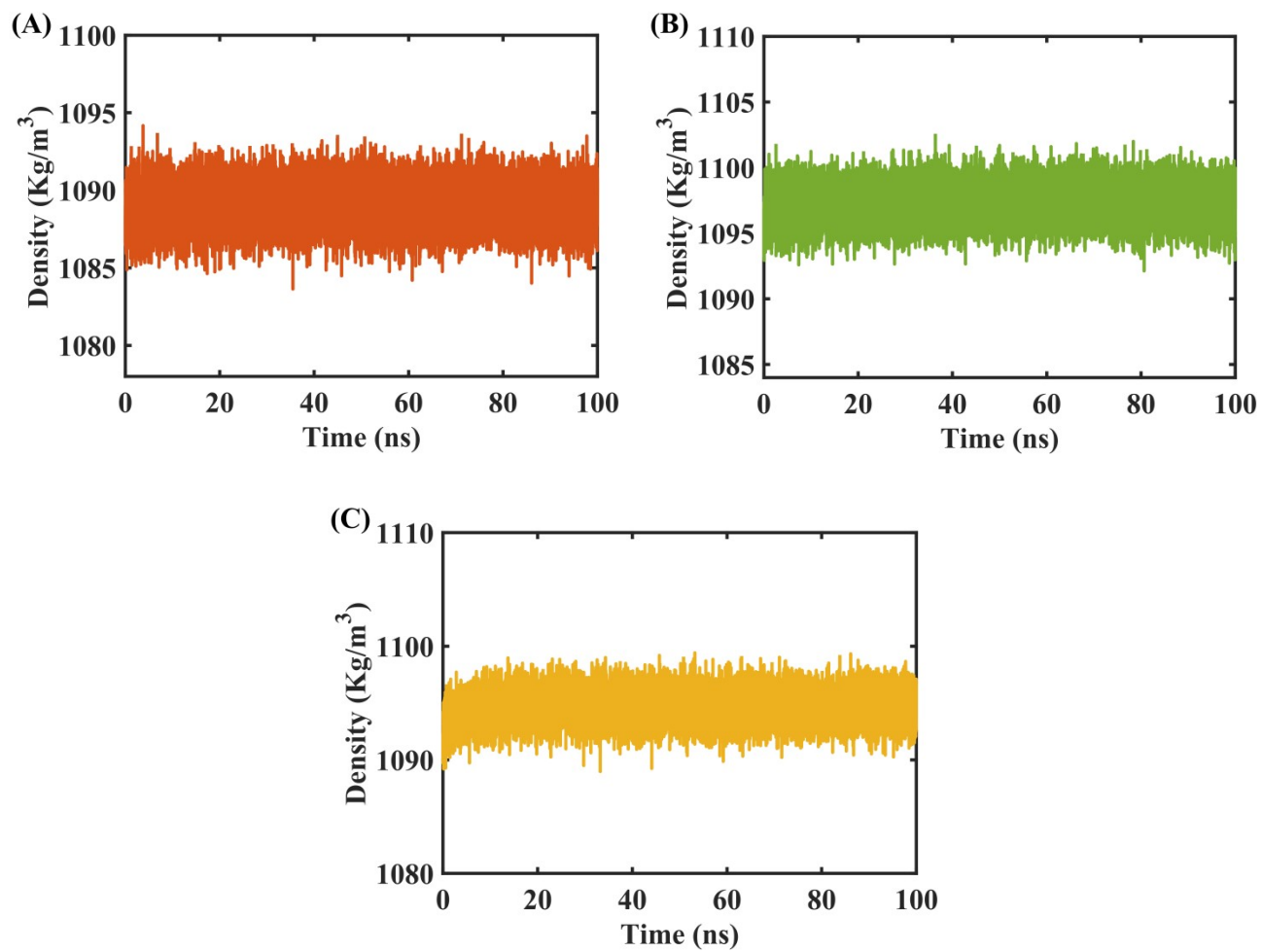


Figure S3 Density of systems containing (A) DNT, (B) RNT, and (C) RDHNT.

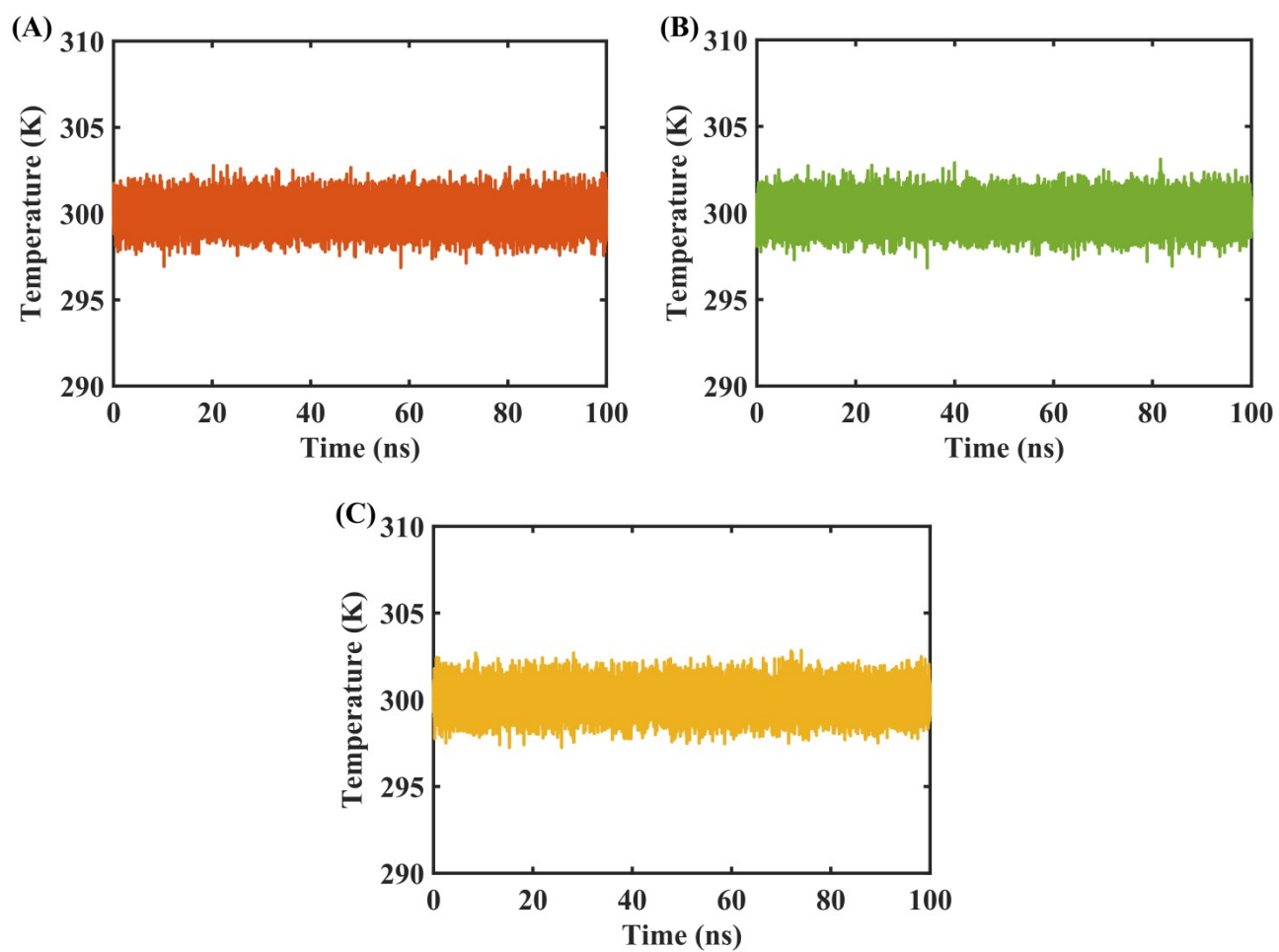


Figure S4 Temperature of systems containing (A) DNT, (B) RNT, and (C) RDHNT.

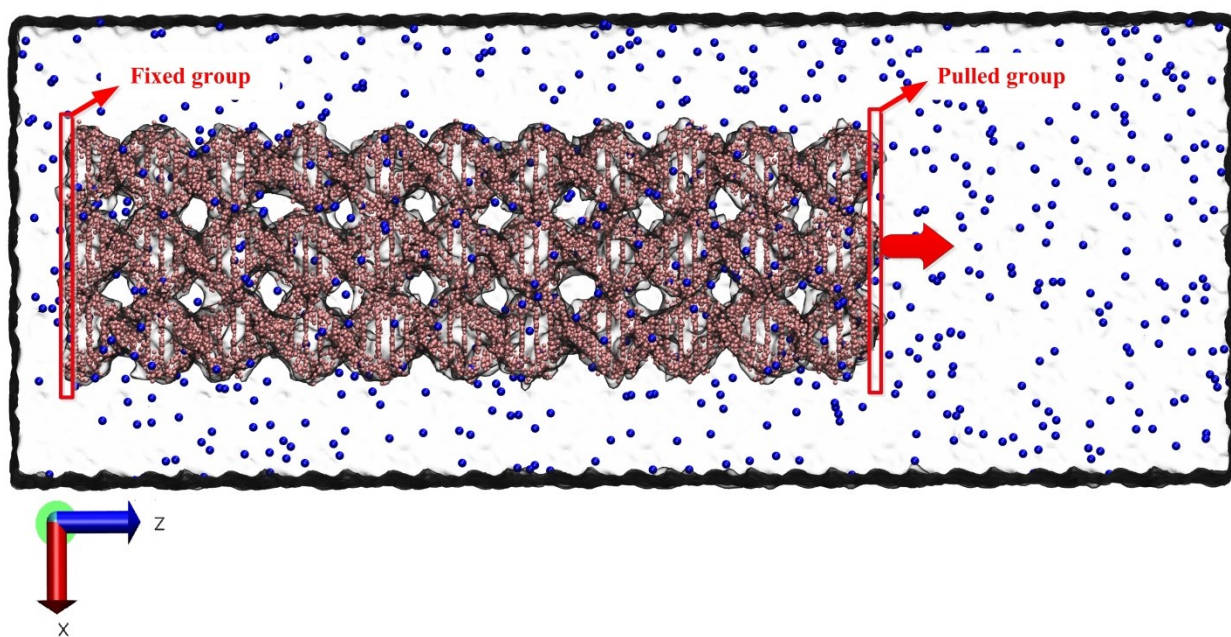


Figure S5 Atomistic structure of a nucleic acid nanotube subjected to tensile force.

Table S3 Details of the simulated systems in non-equilibrium SMD simulations.

Structure	Box size (nm ³)	No. of water molecules	No. of Na ⁺ molecules	No. of total atoms
DNT	10×10×28	83924	656	273704
RNT	10.5×10.5×28	93729	656	303419
RDHNT	10.5×10.5×28	93767	656	303434

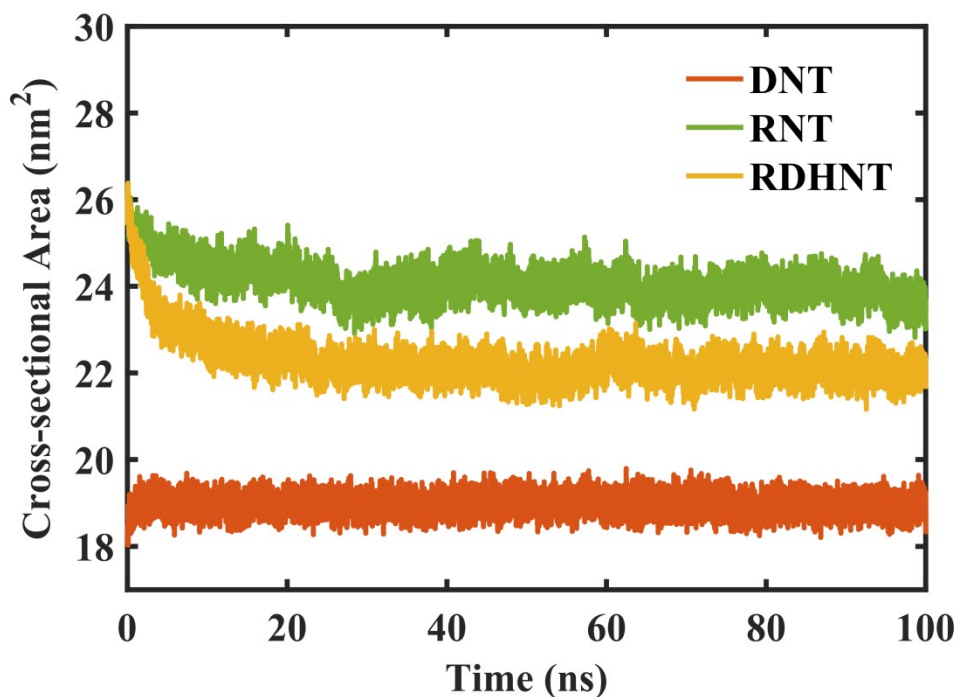


Figure S6 Variations in cross-sectional area over time for DNT, RNT, and RDHNT. The cross-sectional area was calculated by dividing the nanotube's volume by its contour length, using the formula $A=V(t)/L_c(t)$.

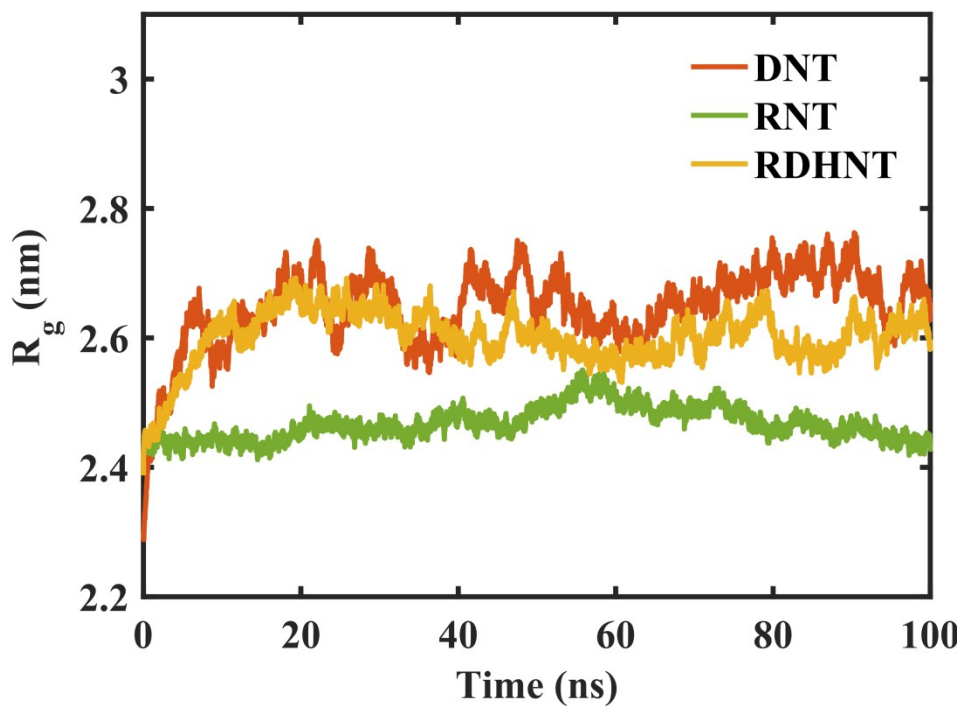


Figure S7 The time evolutions of the radius of gyration (R_g) for nucleic acid nanotubes.

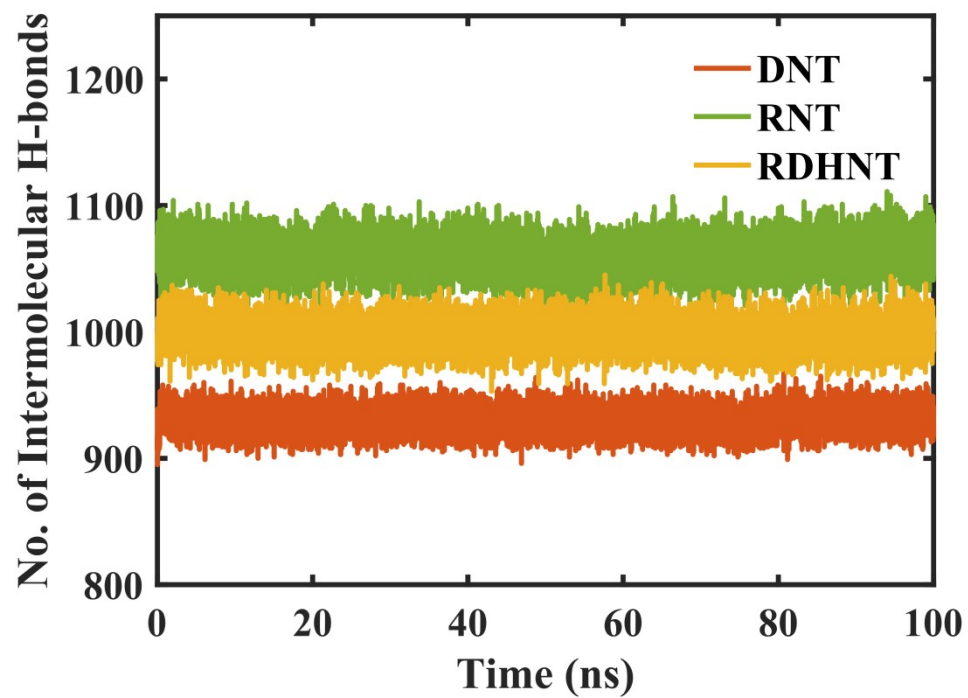


Figure S8 The number of intermolecular hydrogen bonds in DNT, RNT, and RDHNT versus time.

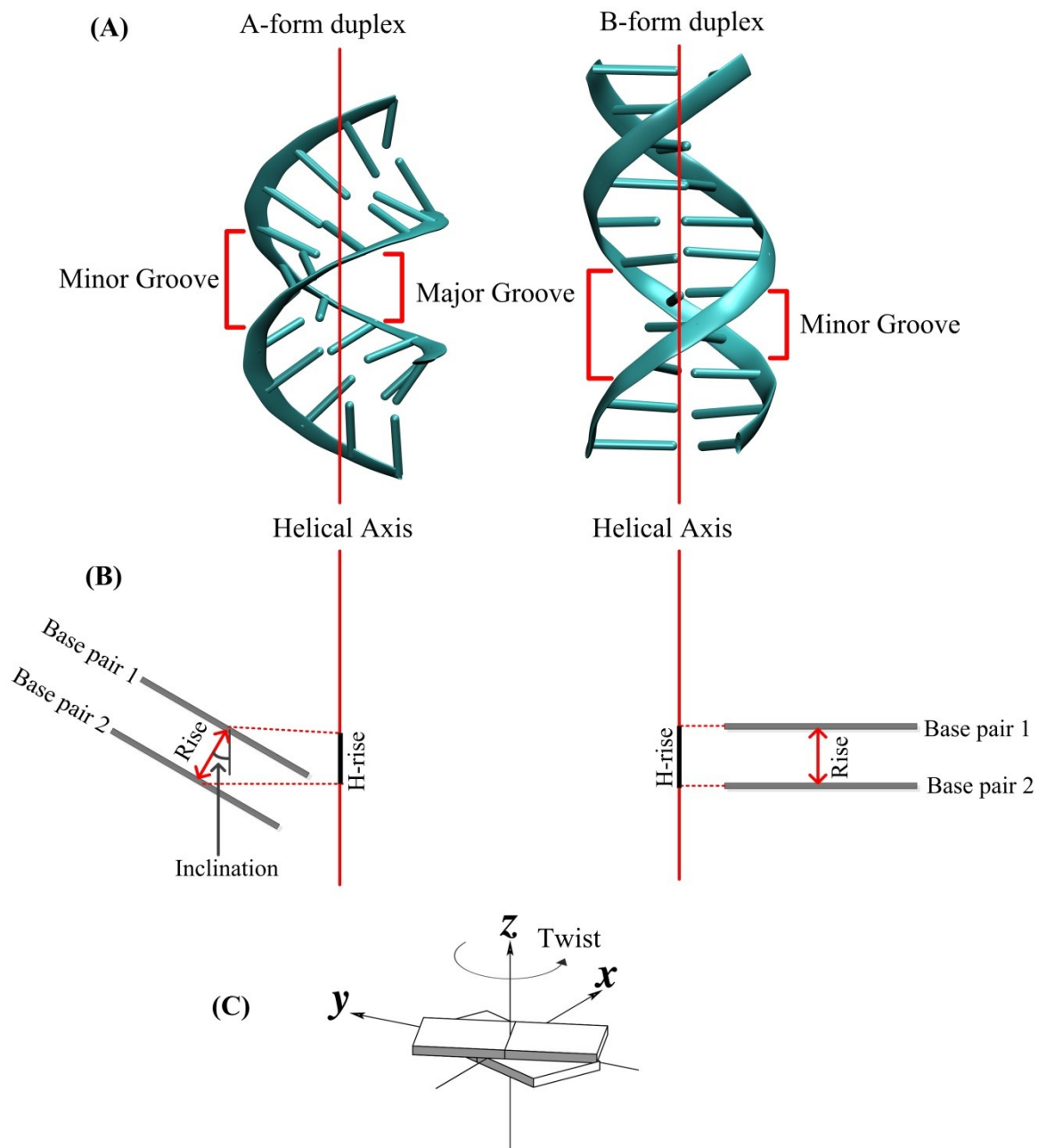


Figure S9 (A) schematics of A-form and B-form duplexes showing major and minor grooves, (B) examples of rise, H-rise, and inclination between consecutive base pairs, and (C) an illustration of the twist between two adjacent base pairs.

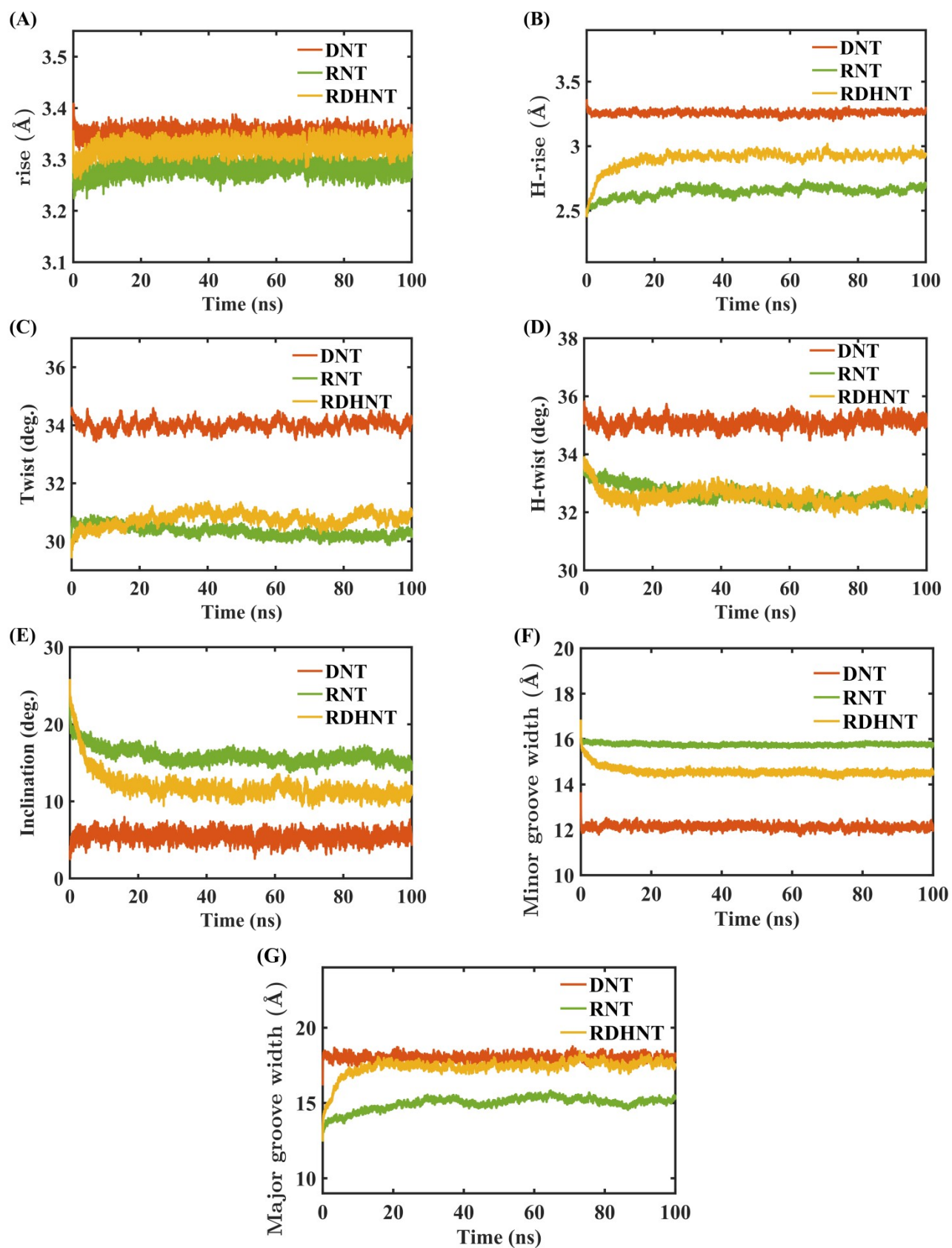


Figure S10 The time evolutions of base pair morphology and groove parameters, including (A) rise, (B) H-rise, (C) twist, (D) H-twist, (E) inclination, (F) minor groove width, and (G) major groove width.

Table S4 The average values of base pair morphology and groove parameters for the initially built structures of DNT, RNT, and RDHNT. The current table also displays the average values derived from the PDB database for DNA, RNA, and RNA-DNA hybrid duplexes.

Microscopic parameter	Initially built structure			PDB database		
	DNT	RDHNT	RNT	DNA	RNA-DNA hybrid	RNA
Rise (Å)	3.4	3.29	3.29	3.36±0.22	3.27±0.18	3.14±0.16
H-rise (Å)	3.35	2.51	2.51	3.25±0.34	2.84±0.24	2.54±0.68
Twist (deg.)	34.34	29.90	29.90	35.85±4.09	32.02±3.01	31.58±8.57
H-Twist (deg.)	35.02	33.49	33.49	36.09±5.12	33.13±1.45	32.94±7.49
Inclination (deg.)	3.62	24.63	24.63	3.74±3.99	11.33±10.87	20.03±8.45
Major groove width (Å)	17.87	13.04	13.04	17.34±0.74	16.11±1.64	13.11±1.2
Minor groove width (Å)	12.39	16.32	16.32	10.92±1.5	15.18±0.28	15.56±0.32

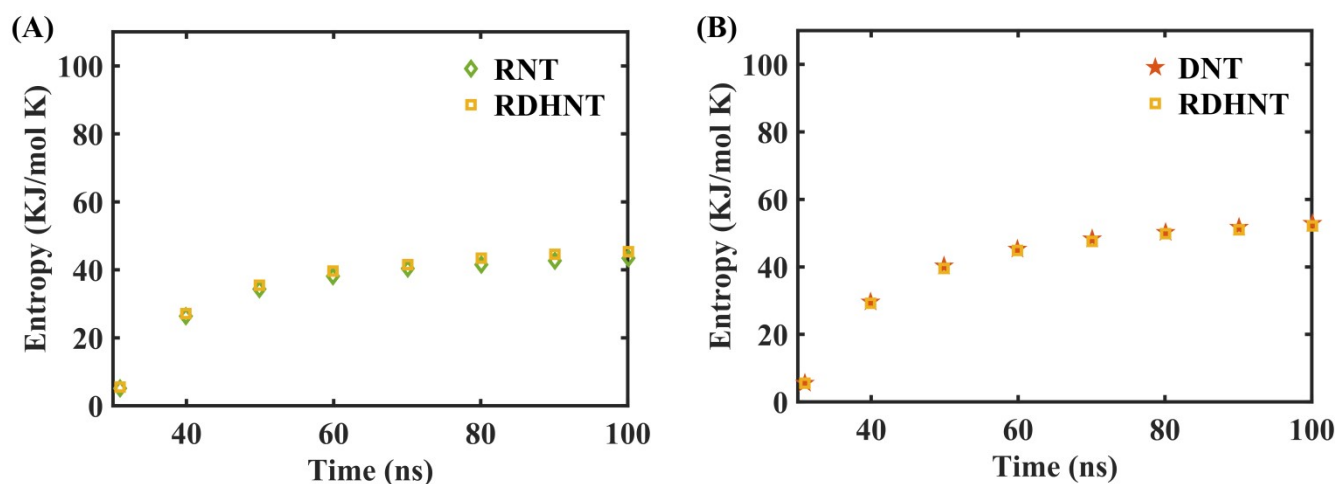


Figure S11 The temporal evolution entropies of (A) RNA scaffolds in RDHNT and RNT and (B) DNA staples in RDHNT and DNT.

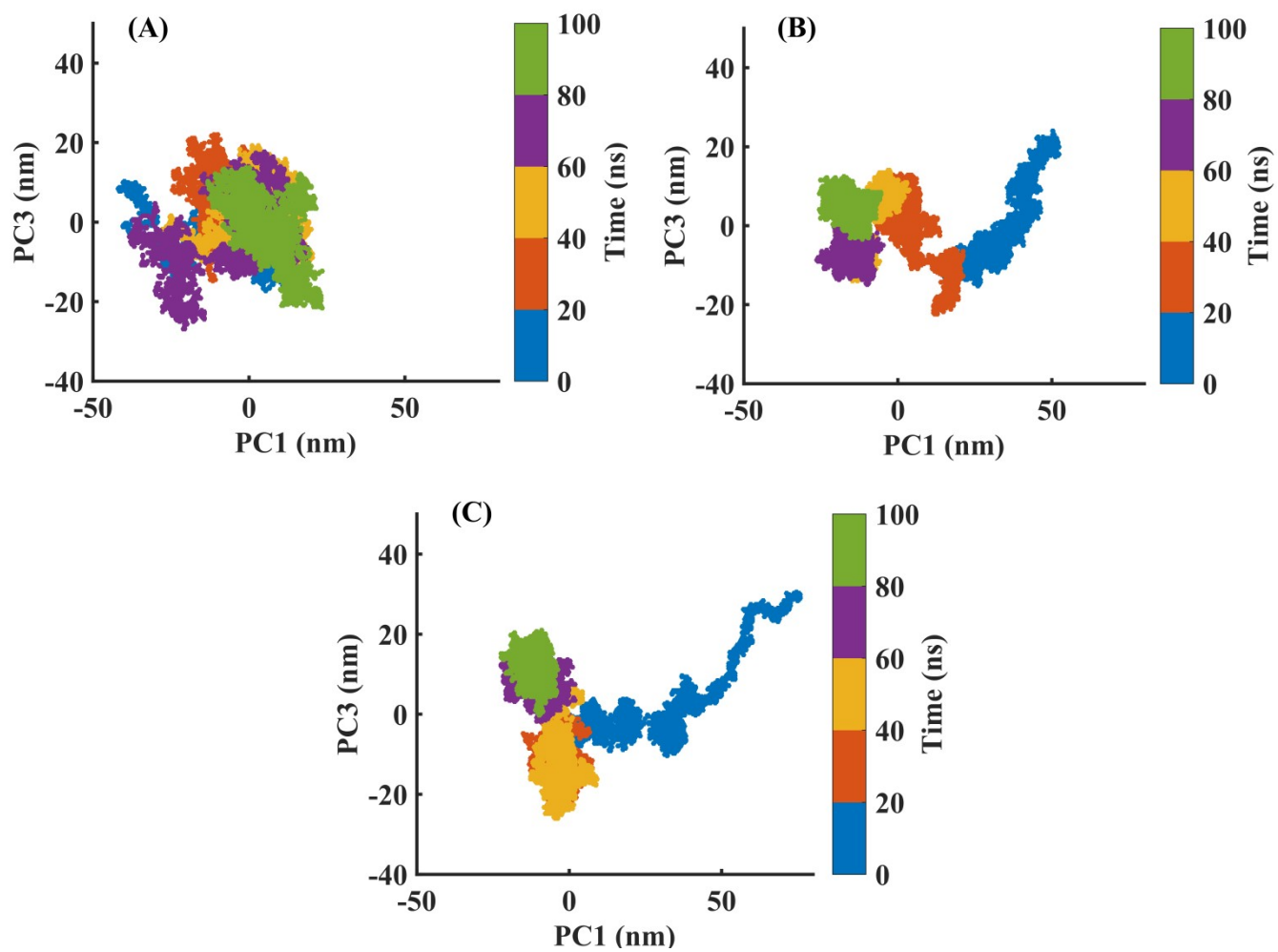


Figure S12 Projection of trajectories along the first and third principal components in phase space for (A) DNT, (B) RNT, and (C) RDHNT.

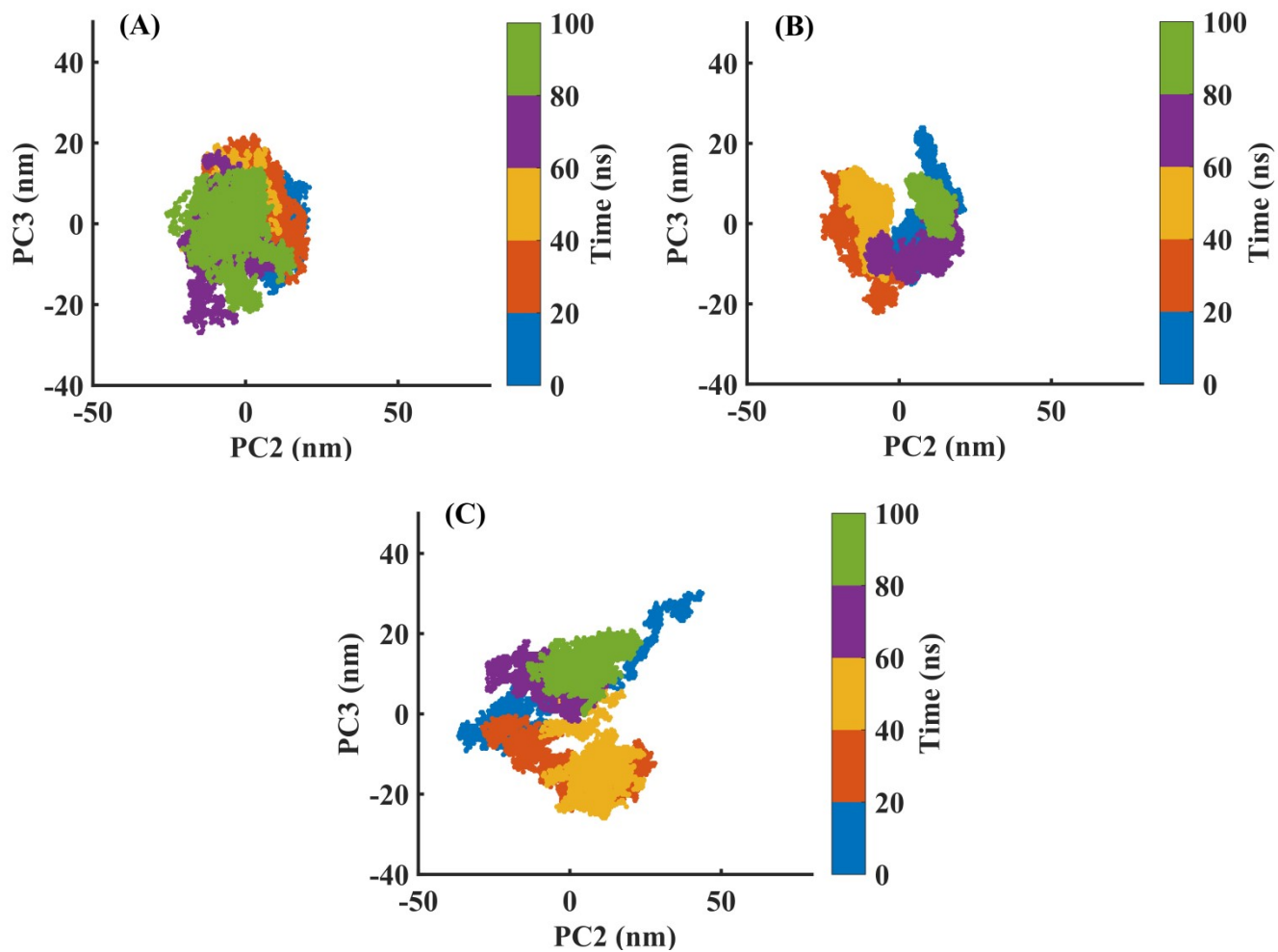


Figure S13 Projection of trajectories along the second and third principal components in phase space for (A) DNT, (B) RNT, and (C) RDHNT.

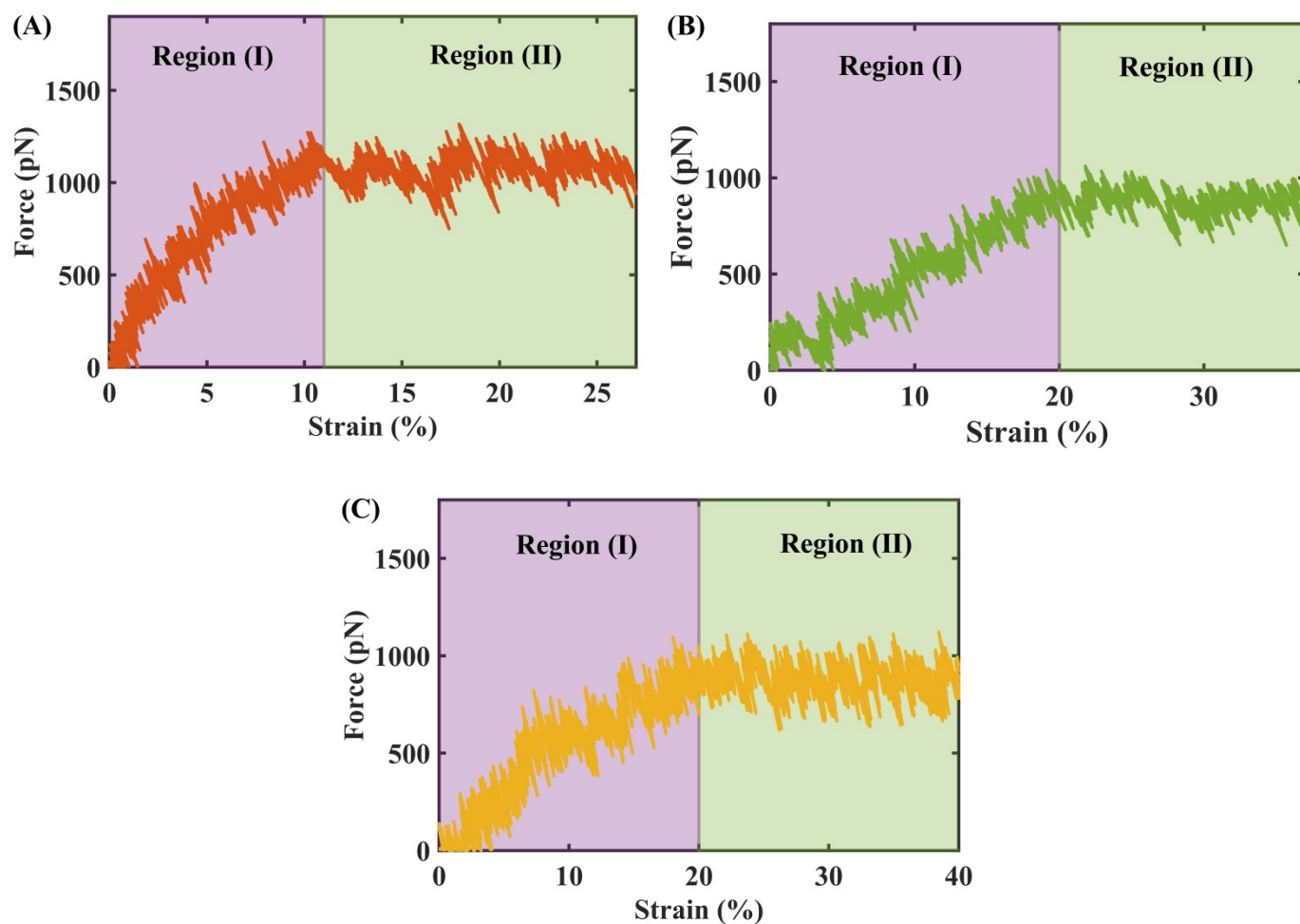


Figure S14 Force-strain graphs obtained from SMD simulations for (A) DNT, (B) RNT, and (C) RDHNT. A velocity of $0.0001 \text{ nm.ps}^{-1}$ was used for these simulations.

Table S5 Tensile stiffness, Young's modulus, yield force, and yield strain obtained from SMD simulations for DNT, RNT, and RDHNT. A velocity of $0.0001 \text{ nm.ps}^{-1}$ was used for these simulations.

Structure	Tensile stiffness (pN)	Young's modulus (MPa)	Yield force (pN)	Yield strain (%)
DNT	7472 ± 53	382 ± 28	1117 ± 80	11 ± 1.8
RDHNT	4307 ± 83	194 ± 34	881 ± 50	20 ± 1.2
RNT	3993 ± 42	174 ± 19	886 ± 95	20 ± 1.3